GEOPHYSICAL RESEARCH LETTERS, VOL. 20, NO. 22, PAGES 2539-2542, NOVEMBER 19, 1993

AASE-II OBSERVATIONS OF TRACE CARBON SPECIES DISTRIBUTIONS IN THE MID TO UPPER TROPOSPHERE

B. E. Anderson[1], J. E. Collins[2], G. W. Sachse[1], G. W. Whiting[3], D. R. Blake[4], F. S. Rowland[4]

Abstract. We report tropospheric (altitudes > 5 km) observations of CO_2, CO, CH_4, and light hydrocarbons (C2 - C4) over the latitude range from 90°N to 23°S recorded onboard the NASA DC-8 aircraft during the winter 1992 Second Airborne Arctic Stratospheric Expedition (AASE-II). Mixing ratios for these species exhibited significant north-south gradients with maximum values in subpolar and arctic regions and minima over the southern tropics. At latitudes > 40°N, the mixing ratios of most species increased significantly over the course of the 3-month measurement period. Also at high northern latitudes, the variations of all relatively long-lived reactive carbon species were linearly correlated with fluctuations of CO_2 with CO, CH_4, C_2H_6, C_2H_2, C_3H_8, and n-C_4H_{10} exhibiting average enhancement ratios in terms of ppbv(X)/ppmv(CO_2) of 13.8, 8.4, 0.21, 0.075, 0.085, and 0.037, respectively.

Introduction

Carbon dioxide and reactive trace carbon gases play important roles in regulating global tropospheric composition and climate [i.e., Logan, 1981; Liu et al., 1987]. As examples, the oxidation of CO is a major global-scale sink for OH [i.e., Logan, 1981]; CO_2 and CH_4 are noted greenhouse gases; and non-methane hydrocarbons (NMHCs) are potentially significant sources of atmospheric CO [Logan, 1981] and tend to dominate OH radical chemistry in regions close to their emission sources [Liu et al., 1987]. Because of their varying reactivity and widely distributed sources and sinks, background tropospheric mixing ratios of these species, including CO_2, vary considerably with latitude, season, and altitude [i.e., Novelli et al., 1992; Blake and Rowland, 1986; Singh et al., 1988; Blake et al., 1992; 1993]. Mixing ratios generally decrease with increasing altitude near source regions [Singh et al., 1988; Blake et al., 1992] and, except for CO_2 in summer, are greater over continental regions than ocean surfaces [Singh et al., 1988]. Recent studies suggest that the carbon species with combustion-related origins exhibit maximum values in the lower troposphere over the northern mid to polar latitudes during winter [Blake and Rowland, 1986; Steele et al., 1987; Novelli et al., 1992] owing to a greater abundance of anthropogenic sources in the northern midlatitudes, a greater consumption of fossil fuels in winter, and the reduced efficiency of tropospheric removal processes at this time of year.

During AASE-II, in situ CO_2, CO, CH_4, and NMHC measurements were obtained onboard the NASA DC-8 aircraft within the mid to upper troposphere over large spatial regions (23°S to 90°N) during the time period from January through March 1992. Because most previous measurements of these species have been obtained at fixed surface sites [i.e., Novelli et al., 1992], aboard ships [i.e., Singh et al., 1988], or from aircraft within the lower troposphere [i.e. Blake et al., 1992], these data significantly augment the data base for detailing the distributions and secular trends of the more abundant carbon species. The following text describes the observed latitudinal distributions of CO_2, CO, CH_4, and C2-C4 hydrocarbons in the mid to upper troposphere (altitudes above 5 km) and temporal trends observed over the 3-month experiment period. The relationships (correlations) between the reactive carbon species are also examined. The reader is referred to Anderson et al. [this issue] for an overview of the AASE-II mission.

1 - NASA/Langley Research Center, Hampton, VA
2 - Science and Technology Corporation, Hampton, VA
3 - Christopher Newport University, Newport News, VA
4 - University of California at Irvine, Irvine CA

Paper number 93GL01693
0094-8534/93/93GL-01693$03.00

Experimental

The NASA DC-8 was deployed each month from January to March 1992 to underfly regions of the arctic polar vortex. A minimum of five flights were conducted during these monthly deployments including transits from San Jose, California, to Anchorage, Alaska; Anchorage to Stavanger, Norway; Stavanger to Bangor, Maine; and Bangor to San Jose. In addition, survey flights were conducted during January and February to Tahiti (from San Jose) and Puerto Rico (from Bangor), respectively, to investigate the spatial distribution and atmospheric effects of Pinatubo aerosols. Individual flights were 10 to 12 hrs in duration and included sampling both within the troposphere and lower stratosphere (to 12 km altitude).

Trace carbon species were measured aboard the DC-8 using (1) a differential absorption tunable diode laser (TDL) system for CO and CH_4 [Sachse et al., 1991]; (2) a broadband, nondispersive infrared absorption sensor for CO_2; and (3) grab sample collection followed by laboratory analyses using gas chromatographic techniques for NMHCs [Blake et al., 1992; 1993].

The TDL instrument was composed of a 20-m folded path White Cell and individual, cryogenically cooled tunable diode laser/infrared detector pairs for each species of interest. The system provided measurement precisions (2 sigma) of 2% for CO and 7 ppbv (0.5%) for CH_4; the system time constant, determined by the White Cell flushing rate, was 5 to 10 s.

A modified Licor model 6252 nondispersive infrared monitor was used to determine CO_2 mixing ratios. This dual cell instrument achieves high precision by measuring the differential absorption between sample air and a calibrated reference gas. The system was operated at constant pressure (225 Torr) and had a precision of 0.05 ppmv (1 sigma) and accuracy of 0.3 ppmv; the system response time (determined by sample flow rate) was 5 to 10 s.

The TDL and CO_2 instruments shared a sampling system consisting of a 0.5-cm diameter, window-mounted sample inlet; $Mg(ClO_4)_2$ filter for removing water vapor; and a compressor for increasing sample pressures to above 225 Torr. Calibrations were performed at about 15-min intervals by introducing NOAA/CMDL standard reference gases to flow upstream of the drying filter. Data were recorded at 1-s intervals and are archived as 5-s averages.

Blake et al. [1992; 1993] describe the general procedures used for collecting grab samples and their subsequent analysis for hydrocarbon species. In brief, a metal bellows pump was used to fill and pressurize to 3 atm a series of evacuated, 2-liter stainless steel canisters with ambient air extracted from a window mounted inlet. Samples were collected at 5- to 10-min intervals during level flight and at about 2-min intervals during vertical profiles; in general, 72 samples were collected per

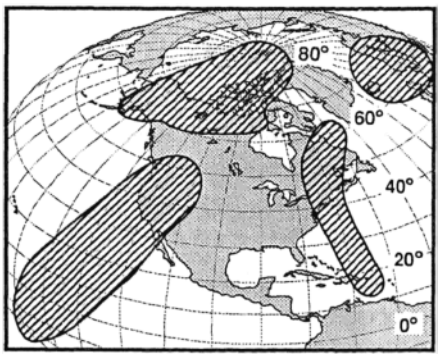

Fig. 1. Map showing the DC-8 tropospheric sampling locations (hashed regions).

flight. The canisters were subsequently shipped to the University of California at Irvine, and samples were cryogenically preconcentrated and analyzed for NMHCs using gas chromatography with flame ionization detection. Mixing ratios were referenced to Scott Specialty Gases (Plumsteadville, PA) and NIST standards. The system has a detection limit of 5 pptv, a precision (± 1 sigma) of 2%, and an accuracy of about 5%. Samples were generally analyzed within 1 to 2 weeks after collection.

Tropospheric data were extracted from the overall DC-8 data set using the following procedure. First, all data recorded below 5-km altitude were eliminated to reduce the effects of localized sources and sinks and vertical concentration gradients (e.g., mixing ratios were generally independent of altitude within the mid to upper troposphere). Next, stratospheric data were eliminated by rejecting points with corresponding N_2O values < 309 ppbv (the observed N_2O average within the lower troposphere minus 1 standard deviation). The effects of stratospheric intrusions were reduced by excluding all points with corresponding O_3 values > 90 ppbv. Finally, measurements from any fresh pollution plumes (as judged by enhancements in short-lived hydrocarbon values) were also deleted. The final tropospheric data set includes over 1600, 1-min averaged CO_2, CH_4, and CO observations and about 260 individual hydrocarbon grab sample measurements; the geographic area represented by this data set is shown in Figure 1.

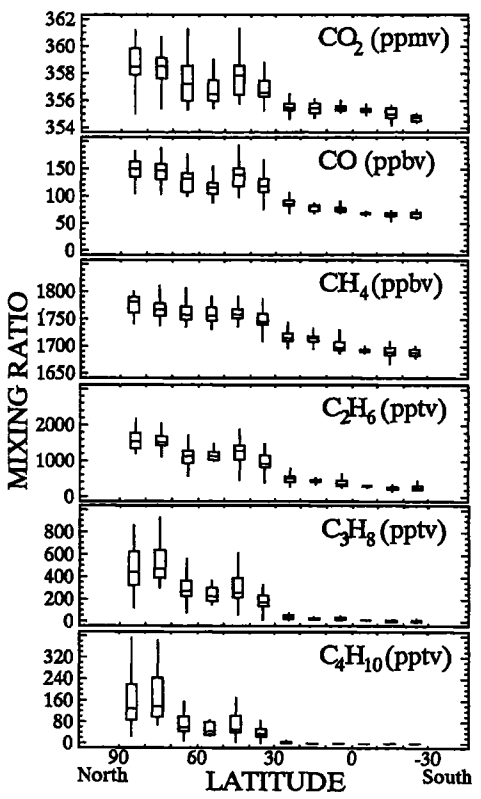

Fig. 2. Plots illustrating the distribution of selected carbon species as a function of latitude. On these types of graphs, median values are represented by the horizontal lines, the upper and lower inner quartiles (75th and 25th percentiles) are enclosed by the boxes, and the vertical lines extend over the data range, or in the case of widely outlying points, to 1.5 times the corresponding inner quartile distance.

Results and Discussion

Figure 2 shows the observed tropospheric distributions of carbon dioxide (CO_2), methane (CH_4), carbon monoxide (CO), and the straight chain hydrocarbons, ethane (C_2H_6), propane (C_3H_8), and n-butane (n-C_4H_{10}) as a function of latitude. Table 1 gives averages and statistics for these species plus ethene (C_2H_4) and ethyne (C_2H_2) in four discrete latitude bands representing the southern tropical(< 0°S), northern subtropical (10°N-30°N), northern subpolar (40°N-60°N), and arctic (>70°N) air mass regions. The various latitude/air mass groupings above 40°N have approximately the same contributions of data from the various monthly flight series except for the 50°-60°N latitude bin of Figure 2. January measurements

TABLE 1. Tropospheric mixing ratios and statistics for selected trace gas species over discrete latitude bands. The CO, CH_4, and CO_2 data are from one minute averages whereas the non-methane hydrocarbon data are from individual grab samples. Hyphens appear where values are below detection limits.

Latitude Range	Species	N	Average	Median	σ
70°N	CO_2 (ppmv)	358	357.7	357.8	1.6
to	CO (ppbv)	370	134.2	136.2	21.3
90°N	CH_4 (ppbv)	370	1764	1763	16.5
	C_2H_6 (pptv)	66	1563	1580	402
	C_2H_4 (pptv)	66	45	28	42
	C_2H_2 (pptv)	66	378	380	133
	C_3H_8 (pptv)	66	461	419	224
	n-C_4H_{10} (pptv)	66	149	117	110
40°N	CO_2 (ppmv)	455	357.5	357.5	1.2
to	CO (ppbv)	467	130.8	128.1	19.8
60°N	CH_4 (ppbv)	466	1761	1758	14.6
	C_2H_6 (pptv)	63	1348	1347	275
	C_2H_4 (pptv)	63	44	20	76
	C_2H_2 (pptv)	63	367	345	177
	C_3H_8 (pptv)	63	298	254	121
	n-C_4H_{10} (pptv)	63	75	50	64
10°N	CO_2 (ppmv)	421	355.5	355.5	0.4
to	CO (ppbv)	435	83.6	83.6	8.8
30°N	CH_4 (ppbv)	435	1715	1715	9.2
	C_2H_6 (pptv)	60	585	581	121
	C_2H_4 (pptv)	60	12	11	5
	C_2H_2 (pptv)	60	68	59	40
	C_3H_8 (pptv)	60	40	34	30
	n-C_4H_{10} (pptv)	60	-	-	-
23°S	CO_2 (ppmv)	323	355.2	355.3	0.3
to	CO (ppbv)	323	67.5	68.3	4.1
0°	CH_4 (ppbv)	323	1690	1691	7.1
	C_2H_6 (pptv)	47	370	372	56
	C_2H_4 (pptv)	47	7	7	6
	C_2H_2 (pptv)	47	28	27	7
	C_3H_8 (pptv)	47	14	16	7
	n-C_4H_{10} (pptv)	47	-	-	-

comprise over 90% of the data within this bin, but contribute a maximum of < 45% to any other latitude bin (Figure 2) or grouping (Table 1) north of 40°N. Because, as discussed below, the carbon species mixing ratios increased significantly between the January and later flight series over high northern latitudes, this temporal sampling bias creates an artificial minimum at 50°-60°N in the Figure 2 plots. This temporal bias does not substantially affect the 40° to 60° grouping of Table 1 because this band is dominated by points from between 40°N and 50°N which have a more uniform temporal spread.

Figure 2 and Table 1 data display significant latitudinal gradients, with all species exhibiting maximum values and substantial variability at northern mid to high latitudes and relatively constant, minimum values south of the Equator. Because many of the carbon compounds have both anthropogenic and biogenic origins, this reflects not only the reduced rate of photochemical destruction in the northern regions during winter, but also the preponderance of land mass, human population, and industrial activity in the northern hemisphere.

Figure 2 also suggests that maximum concentration gradients occur between 30°N and 40°N. This latitude band roughly corresponds to the mean wintertime continental position of the polar jet stream which separates the polar and midlatitude air masses [Barrie, 1986]. When in this position, the jet lies south of many large urban and industrialized areas in North America, Europe, and Asia, which results in polar air masses becoming highly polluted. Moreover, northward transport of midlatitude emissions is generally thought to cause the annual "Arctic Haze" phenomena [Barrie, 1986].

Indeed, our observations (Figure 2 and Table 1) suggest mixing ratios for most species were comparable, if not larger, in the arctic (70°N to 90°N) than at mid-northern latitudes (40°N to 60°N). This is apparently not caused by temporal sampling biases or the fact that a larger fraction of the arctic measurements were acquired at a lower average altitude (6.8 km versus 8.6 km for the 40°N to 60°N band) where greater values might be expected. Temporal sampling biases are discussed above, and we note that the criteria used to create the tropospheric data set eliminates measurements from the lower troposphere where steep vertical concentration gradients were observed. However, to confirm the lack of altitude bias, we examined data from narrow height intervals and still found equivalent or larger values in the arctic. For example, CO mixing ratios between 6- and 7-km altitude were 152.7 ± 14.6 ($\pm$ 1 sigma) above 70°N as opposed to 141.7 ± 14.5 between 40°N and 60°N. Novelli et al. [1992] also report larger wintertime CO values at surface sites in the arctic than at mid-northern latitudes. This is possibly caused by a lack of sinks at high northern latitudes coupled with more frequent influx of clean subtropical air masses to the subpolar region.

In terms of individual species, Figure 2 indicates that CO_2 increased about 1% between the Equator and North Pole. The wintertime northern hemisphere CO_2 maximum is caused by reduced vegetative uptake of CO_2 coupled with emissions from northern midlatitude combustion sources. Carbon monoxide also exhibited a substantial increase, rising almost a factor of 2 between the southern tropics and polar regions. This increase is attributable both to the dominating effect of northern midlatitude pollution and the latitudinal gradient in photochemical destruction rates. Novelli et al. [1992] observed a similar CO gradient in surface measurements in the Pacific region and reported an annually averaged concentration difference between 71°N and 14°S of about 90 ppbv.

Methane increased 3 to 4% in going from southern to arctic latitudes. Because continental biogenic sources of CH_4 are relatively inactive during winter, this difference is caused not only by differences in photochemical sink rates, but possibly by midlatitude anthropogenic sources of CH_4 [Conway and Steele, 1989]; this latter speculation is supported by the observed high positive correlations of CH_4 with CO and CO_2 at northern latitudes (see Table 2). Hansen et al. [1989] also reported positive correlations between CH_4 and combustion tracers during winter and suggested that the enhanced levels of CH_4 seen in the arctic during pollution events arise from anthropogenic activities.

The light hydrocarbons, because of their reactivity, exhibited much more pronounced inter-hemispheric gradients than the monocarbon trace species. In going from the Equator to the Arctic, C_2H_6 decreased a factor of 4 whereas C_3H_8 dropped by more than a factor of 25. The shorter-lived species (e.g., C_2H_4 and C_4H_{10}), while present in significant amounts at high northern latitudes, were generally at or below detection limits near the Equator and south. These differences are consistent with previous measurements [i.e., Blake and Rowland, 1986; Singh et al., 1988] and were driven both by the dominating source strength of the northern midlatitudes and the enhanced rates of destruction in the tropics and subtropics associated with the abundant sunlight and moisture.

TABLE 2. Correlation coefficient (r) matrix for measurements recorded at latitudes above 40°N. The regression slopes on CO_2 and CO in units of ppbv (species)/ppmv (CO_2) and ppbv (species)/ppbv (CO) are given for species with respective r values > 0.5. The data base for these calculations is comprised of over 800, one-minute averaged CO_2, CO, and CH_4 data points and about 140 individual hydrocarbon samples.

Species	CO_2	CO	CH_4	C_2H_6	C_2H_4	C_2H_2	C_3H_8	n-C_4H_{10}
CO_2	–	0.94	0.77	0.75	0.40	0.69	0.58	0.52
[slope]	–	13.7	8.4	0.21	–	0.075	0.085	0.037
CO	0.94	–	0.71	0.67	0.59	0.80	0.45	0.40
[slope]	64.2	–	0.55	11	1.3	5.6	–	–
CH_4	0.77	0.71	–	0.75	0.50	0.65	0.75	0.74
C_2H_6	0.75	0.67	0.75	–	0.62	0.85	0.91	0.87
C_2H_4	0.40	0.59	0.50	0.62	–	0.80	0.54	0.57
C_2H_2	0.69	0.80	0.65	0.85	0.80	–	0.67	0.61
C_3H_8	0.58	0.45	0.75	0.91	0.54	0.67	–	0.99
n-C_4H_{10}	0.52	0.40	0.74	0.87	0.57	0.61	0.99	–

As noted above and illustrated in Table 3, the mixing ratios of all species were observed to increase over the course of the winter at mid to high northern latitudes (>40°N). Carbon dioxide, for example, increased about 2.5 ppmv between the January and March flight series which is consistent with its reported late winter/early spring maximum in arctic regions

TABLE 3. Temporal changes in species mixing ratios between the January and March flight series for measurements within the 40°N to 90°N latitude region.

Species	N	Average	Median	σ	Lower Quartile	Upper Quartile
			January			
CO_2 (ppmv)	406	356.4	356.2	0.7	355.9	356.7
CO (ppbv)	406	115.3	114.1	11.6	106.1	119.9
CH_4 (ppbv)	406	1756	1751	14.1	1746	1769
C_2H_6 (pptv)	38	1201	1127	246	1020	1250
C_2H_4 (pptv)	38	31	19	44	15	34
C_2H_2 (pptv)	38	253	226	99	186	281
C_3H_8 (pptv)	38	316	269	151	214	328
n-C_4H_{10} (pptv)	38	87	59	70	37	89
			March			
CO_2 (ppmv)	196	358.9	358.8	0.9	358.3	359.1
CO (ppbv)	213	152.1	152.4	13.8	141.4	161.2
CH_4 (ppbv)	212	1767	1765	15	1757	1777
C_2H_6 (pptv)	79	1529	1494	279	1346	1685
C_2H_4 (pptv)	79	38	24	39	15	47
C_2H_2 (pptv)	79	393	380	113	324	447
C_3H_8 (pptv)	79	377	339	173	246	450
n-C_4H_{10} (pptv)	79	106	85	81	44	138

[Tanaka et al., 1987]. Carbon monoxide also apparently accumulated over the winter at the northern latitudes, increasing by about 30% over the 66-day experiment period. Methane values rose by about 13 pbbv which is comparable to its current globally averaged annual increase. The light hydrocarbons also exhibited substantial temporal increases, consistent with their reported late winter/early spring seasonal maxima [e.g., Blake and Rowland, 1986].

The late winter carbon species mixing ratios above 40°N were also greatly enhanced relative to comparable summertime measurements. For example, our March CO values (Table 3) were about 50% larger than those reported by Talbot et al. [1993] for summertime polar air masses over Canada and Alaska. In addition, the March C_2H_6 and C_3H_8 mixing ratios (see also Table 3) are 2 and 4 times greater, respectively, than those measured by Blake et al. [1993] within summertime background air over Canada. In fact, the March hydrocarbon concentrations in Table 3 are more comparable to values recorded within relatively fresh biomass burning emissions than to summertime background measurements. For example, the March C_2H_6, C_2H_2, and C_3H_8 values are similar to the peak mixing ratios of 1573 pptv, 444 pptv, and 262 pptv, respectively, observed by Blake et al. [1993] in a prominent, 12- to 18-hour old smoke plume over central Canada.

The high positive correlations of Table 2 suggest common causes for the northern latitude wintertime concentration enhancements. The longer-lived species--CO_2, CO, CH_4, and C_2H_6--tend to be well correlated which implies that their enhancements arise from combustion processes (industrial or biomass). The more reactive species--C_3H_8 and n-C_4H_{10}--are extremely well correlated with each other and with C_2H_6 of the group referenced above, which reflects not only their combustion-related sources but similar atmospheric residence times. The enhancement ratios (e.g., regression slopes shown in Table 2) for the reactive species relative to CO_2 vary from 13.7 ppbv(CO)/ppmv(CO_2) down to 0.037 ppbv (n-C_4H_{10})/ppmv-(CO_2); the CH_4/CO_2 enhancement ratio, 8.4 ppbv/ppmv, is within the range reported by Conway and Steele [1989] for winter/spring air masses over North America. More detailed analyses of CO_2, CH_4, and CO concentrations (data not shown) from March soundings over the North Pole indicate an even stronger correlation between CO_2 and CH_4 ($r=0.99$) along with CO_2 and CO ($r=0.99$). Similar high positive correlations between CH_4 and combustion tracers have been observed in Arctic Haze [i.e., Conway and Steele, 1989] where tracer and trajectory analyses [Lowenthal and Rahn, 1985; Hansen et al., 1989] indicate long-range transport of combustion products from Eurasia, in particular from the former U.S.S.R., significantly contributed to the observed trace carbon enhancements.

Conclusion

The AASE-II observations substantially enhance the available base of information on the latitudinal distributions of CO_2 and reactive trace carbon gas distributions in the mid to upper troposphere. Specific results indicate that concentrations are much greater and more variable over the mid to high northern latitudes than within the tropics or subtropics. This reflects both the seasonally reduced rates of photochemical destruction and the greater abundance of biogenic and anthropogenic sources in northern regions. Concentrations within polar and arctic air were also observed to increase between the January and March flight series implying that, because of the reduced efficiency of removal processes, pollutants tend to accumulate in these air masses over the course of the winter. Finally, the fluctuations of most species over mid to high northern latitudes were correlated with those of CO_2 and CO which suggests their enhancements may be caused by combustion-related sources.

References

Anderson, J. G., et al., Geophys. Res. Lett., this issue.

Barrie, L. A., Arctic air pollution: An overview of current knowledge, Atmos. Environ., 20, 643-663, 1986.

Blake, D. R. and F. S. Rowland, Global atmospheric concentrations and source strength of ethane, Nature, 321, 231-233, 1986.

Blake, D. R. et al., Summertime measurements of selected nonmethane hydrocarbons in the arctic and subarctic during the 1988 Arctic Boundary Layer Expedition (ABLE 3A), J. Geophys. Res., 97, 16559-16588, 1992.

Blake, D. R. et al., Effects of biomass burning on summertime nonmethane hydrocarbon concentrations in the Canadian wetlands, J. Geophys. Res., in press, 1993.

Conway, T. J., and L. P. Steele, Carbon dioxide and methane in the Arctic atmosphere, J. Atmos. Chem., 9, 81-100, 1989.

Hansen, A. D. A., et al., Correlations among combustion effluent species at Barrow, Alaska: Aerosol black carbon, carbon dioxide, and methane, J. Atmos. Chem., 9, 283-299, 1989.

Liu, S. C., et al., Ozone production in the rural troposphere and the implications for regional and global ozone distributions, J. Geophys. Res., 92, 4191-4207, 1987.

Logan, J. A., Tropospheric ozone: Seasonal behavior, trends, and anthropogenic influence, J. Geophys. Res., 90, 10463-10482, 1981.

Lowenthal, D. H., and K. A. Rahn, Regional sources of pollution aerosol at Barrow, Alaska during winter 1979-80 as deduced from elemental tracers, Atmos. Environ., 19, 2011-2024, 1985.

Novelli, P. C., et al., Mixing ratios of carbon monoxide in the troposphere, J. Geophys. Res., 97, 20731-20750, 1992.

Sachse, G. W., et al., Airborne tunable diode laser sensor for high-precision concentration and flux measurements of carbon monoxide and methane, Proc. SPIE Int. Symp. on Laser Spec., Los Angeles, CA, Jan. 20-25, 1991.

Singh, H. B., et al., Measurements of selected C_2-C_5 hydrocarbons in the troposphere: Latitudinal, vertical, and temporal variations, J. Geophys. Res., 93, 15861-15878, 1988.

Steele, L. P., et al., The global distribution of methane, J. Atmos. Chem., 5, 125-171, 1987.

Talbot et al., Summertime distributions and relations of reactive nitrogen species and NO_y in the troposphere over Canada, J. Geophys. Res., in press, 1993.

Tanaka, M., et al., Seasonal and meridional variations of atmospheric carbon dioxide in the lower troposphere of the northern and southern hemispheres, Tellus, 39B, 29-41, 1987.

B. E. Anderson, Mail Stop 483, NASA/Langley Research Center, Hampton, VA 23681.

D. R. Blake, Department of Chemistry, University of California-Irvine, Irvine CA 92717.

J. C. Collins, Mail Stop 468, NASA/Langley Research Center, Hampton VA 23681.

F. S. Rowland, Department of Chemistry, University of California-Irvine, Irvine CA 92717.

G. W. Sachse, Mail Stop 468, NASA/Langley Research Center, Hampton, VA 23681.

Recieved: March 5, 1993;
accepted: June 11, 1993